Infrared Absorption Spectroscopy of Carbon Monoxide Trapped in Solid Hydrogen Matrix

YAN, Lei

A Thesis Submitted in Partial Fulfillment
of the Requirements for the Degree of
Master of Philosophy
in
Chemistry

Thesis Committee

Prof. Zhifeng Liu (Chair)

Prof. Sik Lok, Lam (Committee Member)

Prof. Man-Chor Chan (Thesis Supervisor)

Abstract

The study of the high-resolution infrared (IR) absorption spectra of carbon monoxide molecules embedded in matrices of para-hydrogen crystals was presented. The narrow line widths observed in solid parahydrogen promises the possibility of using this system as a matrix material for high resolution spectroscopy to study anisotropic intermolecular interactions in the condensed phase. In this thesis, experimental studies along this line are reported. In the system of CO-doped solid parahydrogen crystals, sharp lines presumably due to rotational structure were observed. The effect of orthohydrogen and CO concentration were investigated. Based on these observation, a preliminary analysis of the spectrum will be discussed.

摘要

在過去的兩年中，我們搭建了一套用於基質隔離高分辨紅外吸收光譜的實驗儀器，基質材料爲固態仲氫，而研究的對象是一氧化碳分子。因爲固態仲氫作爲基質隔離材料有很多獨特的優點，所產生的光譜具有線寬很窄的特點，使得我們可以研究和分辨基質中摻雜分子和氫分子的相互作用，並提供豐富的關於摻雜分子結構和動力學資訊。這些資訊有助於我們研究基質隔離體系中分子間的不均一勢能。在這篇論文裏，基質隔離的相關背景和實驗的相關細節以及一氧化碳分子在固態仲氫氣基質中振動和轉動結構得到詳細闡釋和說明。

Acknowledgements

I would like to express my pure-hearted gratitude to all those who gave me the possibility to complete this thesis, especially my supervisor Prof. M. C. Chan. In the past two years study under Prof. Chan's kind guidance, what I have learned is not only the experimental techniques and theoretical knowledge, but also the enthusiasm to the scientific research. He is full of passion and energy, even when he faces blows and obstacles, and then solutions always came out of his mind. What is more, he is a gentle man with many humors and his amiable personality make him very easy to stay with. I will always remember encourages he gave to me when I encountered the heavy frustration in my study and living of my early days in Hong Kong. It was him that helped me out of the trouble and established my self-confidence. I would say that I can not accomplish my M. Phil study without his encouragement and help.

I would also not forget my groupmates for their very kind supporting. I have learned a lot from discussions with Mr. Fangyuan Han, and received many suggestions not only on study, but also on living, from Miss. Yan Song and Miss. Jun Liu. Their selfless help contribute my advancement.

Beside that, the staff and fellows from other research groups and

technical supporting unit, also gave me a lot of supporting and suggestions which made my research progress much more smooth. Thanks also come to them.

At last, but most important, I cannot forget to mention my family members-my mother, my father and my girlfriend. Their deep love and care in every possible way cannot be expressed by any word in the world. I will dedicate this thesis to them.

Table of Contents

Chapter I. Introduction

Spectroscopy of matrix-isolated molecules was first introduced by Lewis.[1] This approach involves spectroscopic studies of molecules trapped in a rigid and chemically inert "cage" of solid matrix materials at cryogenic temperature. Matrix isolation spectroscopy opens a new direction of studying reactive species.[2] The low temperature minimizes the motions of isolated species. Furthermore, the inert matrix environment minimizes the reactivity of the isolated species, resulting in prolonged lifetime.[3] The much higher density in the solid state compared to the gas phase should in principle improve dramatically the detectability of the isolated species. From a technological point of view, the matrix serves as a long time integrating detector in which chemical species can be collected by deposition, or built up *in situ*, to a readily detectable level. Hence, matrix isolation spectroscopy has been employed in a variety of analytical and diagnostic applications.[3] The structural and spectroscopic properties of numerous previously unknown chemical species, including free radicals and transient intermediates, have been characterized by matrix isolation spectroscopy.[4] These studies in many cases guide the way for the corresponding gas phase studies, yielding new insights into chemical reaction mechanisms. Matrix-isolated species provide model systems for understanding the role of many-body interactions in various physical and chemical processes as well as the quantum effect in the more complex condensed phase with high

number density and low temperatures achieved in a matrix environment.

On the other hand, matrix isolation spectroscopy displays a number of limitations. Compared to the case in the gas phase, spectral transitions in the solid state suffer homogeneous and inhomogeneous broadening that wash out the detailed rovibrational structures.[5] The typical observed spectral width is on the order of a few cm^{-1}. The homogeneous broadening arises from strong intermolecular interactions in the solid state. The inhomogeneous broadening arises from the various microscopic environment surrounded the isolated species as well as the possible amorphous structure in the solid matrix. In addition, matrix-isolated molecules may have limited degree of freedom for internal motion due to strong intermolecular interactions. It is common that only vibrational transitions are observed in matrix spectroscopy without any rotational structure.[6] This makes the identification of unknown species more difficult in case the corresponding gaseous data is unavailable.

As demonstrated by numerous observations since the 1980s, solid parahydrogen is a unique system for matrix spectroscopy.[7-12] While considered the simplest molecular solid, solid H_2 distinguishes itself from other traditional matrix materials such as Ne, Ar, Kr, Xe and N_2 by a variety of properties arising from the combination of small molecular size, large intermolecular separation, and weak intermolecular interactions.[13] Due to the large separation and weak intermolecular interactions, molecules are only slightly perturbed in solid H_2 compared to the gas state. The properties can therefore be elucidated based on

first principles. The narrow linewidth observed in systems of solid hydrogen allows the rovibrational structure (as well as crystal field splitting due to anisotropic interactions in some cases) to be resolved. As a result, quantitative analysis of the spectra becomes possible. By analyzing the fine structure in the rovibrational spectra, one can obtain a wealth of information on selection rules, intermolecular interactions, as well as relaxation process.

During my residence as an M. Phil. student, I was involved in setting up an experiment to study the rovibrational spectroscopy of molecules in parahydrogen matrix. In addition to building the apparatus, the infrared spectrum of CO molecules in parahydrogen was also studied. The details of this work are presented in this thesis. To date, however, our observations provide more questions than answers. While we have not completely understood the observed features, a qualitative assignment has been made. More systematic experimental work is needed to give a quantitative analysis.

In the rest of the thesis, we will discuss the properties of hydrogen in Chapter Ⅱ, followed by the experimental details in Chapter Ⅲ. The work of CO will be presented in Chapter Ⅳ. This thesis concludes with Chapter Ⅴ, where an outlook will also be given.

Chapter II. Properties of Hydrogen

Hydrogen molecules H_2 are composed of two protons separated by about 0.74 Å surrounded by two electrons, forming one of the simplest diatomic molecules. Because of its simplicity, H_2 and its isotopmers have been served as model systems for testing high-level *ab initio* calculations. Over the years, properties of hydrogen have been extensively studied and well documented elsewhere.[14] Table I[15] lists some of the physical properties. To aid our discussion in the following chapters, some spectroscopic properties of hydrogen are reviewed here.

A. Spectroscopic Properties of Hydrogen Molecules

Due to the coupling of the two spin-1/2 protons, the total nuclear spin I in H_2 molecules is either 1 or 0, corresponding to two protons with parallel or anti-parallel spins. According to the Pauli principle, molecules with I=0 can only occupy states with rotational quantum number J = even while molecules with I=1 can only occupy states with rotational quantum number J = odd. According to the quantum theory of angular momentum, there are $2I$+1 allowed M_I states for each I value. The I=1 species has therefore three allowed states while the I=0 species has only one. Thus, the I=1 species is three times as abundant as the I=0 species at room temperature. Since the conversion of nuclear spin is strictly forbidden by the parity consideration under the adiabatic approximation

Table I Tabulated physical properties of hydrogen

Molecular weight	2.0157
Normal boiling point	20.278 K
Density at normal boiling point	0.07087 g/cm^3
Triple point	13.813 K
Pressure at triple point	52.82 Torr
Density at triple point	0.07709 g/cm^3
Critical point	32.976 K
Pressure at critical point	$9.6976\times10^{}$ Torr
Density at critical point	0.03145 g/cm^3
Heat of vaporization	$4.459\times10^{}$ erg/g
Heat of fusion	$5.82\times10^{}$ erg/g
Specific heat	$9.67\times10^{}$ erg/g
Thermal conductivity	$11.8\times10^{}$ erg/cm s K
Viscosity	135.4 micropoise
Surface tension	$1.93\times10^{}$ dyne/cm
Dielectric constant	1.2285
Molar volume of solid at 4.2 K	
99.8% p-H_2	23.064 cm^3/mole
n-H_2	22.820 cm^3/mole

only extremely slow nuclear spin conversion results from the breakdown of adiabatic approximation. In effect, H_2 molecules with different nuclear spin behave as different species. They are often referred as nuclear spin modifications. Traditionally, the more abundant nuclear spin modification is termed ortho, and the less abundant one para. In the case of H_2, parahydrogen is the species with even J and I=0 and orthohydrogen is the species with odd J and I=1.[8]

Due to the slow nuclear spin conversion,[7] the ortho/para ratio of 3 to 1 remain unchanged when H_2 is cooled from room temperature to cryogenic temperature. On the other hand, the Boltzmann distribution implies that only the J=0 rotational state is effectively populated by the parahydrogen p-H_2 (p-H_2), while the J=1 rotational state is populated by the orthohydrogen o-H_2 (o-H_2). The relaxation from the J=1 state to the J=0 state is negligible in the solid phase[8] under normal pressure. In other words, o-H_2 is a metastable species with extremely long lifetime in the solid state. The conversion between o-H_2 and p-H_2 can be catalyzed by a paramagnetic material, which provides a non-uniform magnetic field. The detailed discussion of ortho/para conversion will be given in Chapter III.

Like other homonuclear diatomic molecules, H_2 has no permanent or vibration-induced dipole moment. As a result, pure rotational and rovibrational transitions are forbidden by the dipole mechanism. On the other hand, transitions via quadrupole mechanism and Raman scattering have been

observed.[13] In addition, transitions due to intermolecular interactions have also been observed in high pressure gas as well as in the condensed phase.[16]

B. Properties of Solid Hydrogen

Properties of solid hydrogen have been extensively studied in many aspects for years.[7,8,13] It has been known that H_2 crystals are formed in either hexagonal close-packed or face-centered cubic structures, with the nearest neighbor distance of 3.79 Å. As the simplest and most fundamental molecular solid, molecules in crystals of H_2 retain their identity with properties not too different from those in the gas phase. Interactions in solid p-H_2 are mainly isotropic dispersion interactions. Since the J=0 rotational wavefunction has a spherical shape, parahydrogen molecules at the J=0 state have no permanent electric moments of any order. In other words, anisotropic interactions is absent in pure p-H_2 crystals. On the other hand, o-H_2 molecules occupying the J=1 rotational quantum number have a small permanent quadrupole moment. As a result, the small o-H_2 concentration in para-enriched H_2 crystals leads to the electric quadrupole-quadrupole (EQQ) interactions, the most dominant anisotropic interactions in the crystal.

Properties of solid hydrogen are dominated by quantum effects, arising from the combination of small molecular size (0.74 Å), large lattice constant, and weak intermolecular interactions. Solid H_2 is an exceptionally soft crystal. The density of the crystal is doubled from its zero pressure value by applying a

pressure of 20 Kbar, whereas such pressure change only results in a few percent increase in other solids.[15] Like He, solid hydrogen is considered translational quantum crystal that is signified by the large compressibility. In addition, solid H_2 exhibits large amplitude of zero-point lattice vibration.[17] The mean amplitude of the zero-point lattice vibration in solid p-H_2 amounts to almost 20% of the nearest intermolecular distance. Molecules are therefore not sharply located at the equilibrium lattice sites. Because of these properties, impurity molecules with size much greater than that of H_2 can fit into the lattice sites of solid H_2 without causing much crystal defect. Solid H_2 under ultrahigh pressure (>200 G Pa) exhibits very rich phases that may be related to the long predicted metallic transition.

Solid hydrogen displays unusually high thermal conductivity which may be ascribed to its large zero-point lattice vibration.[18] The thermal conductivity of para-enriched solid hydrogen containing 0.2% o-H_2 is 50 $Wm^{-1}K^{-1}$ at 4.2 K,[7] which is comparable to that of Cu, and is almost one order of magnitude greater than those of rare gas crystals.[3] The high thermal conductivity of solid parahydrogen allows fast thermal exchange with the surroundings. This property is particularly important for the annealing process of matrix material. For instance, the fast dissipation of excess energy produced in the photolysis of molecules in solid H_2 is crucial in stabilizing the photofragments in the H_2 crystal.

Molecule in solid H_2 is only slightly perturbed by the solid state

environment as shown in numerous experiments.[19-21] Molecules in solid H_2 are expected to have internal motions (such as rotation and vibration) like in the gas phase. Based on thermodynamic considerations, Pauling predicted the hindered rotation of H_2 in the solid.[22] Rovibrational spectra of solid H_2 were observed in the 1950s. The spectral pattern of the spectra indicates that H_2 molecules have nearly free rotation and vibration. As a result, both J and v remain good quantum numbers. The weak anisotropic intermolecular interactions, on the other hand, give rise to the fine structures in the spectra. These interactions are also responsible for many other observed effects such as multipole-induced dipole and relaxation processes.

In forming a para-enriched H_2 crystal from the gas state, the spatial distribution of metastable o-H_2 molecules is expected to be completely random. On the other hand, the EQQ interaction between pairs of o-H_2 molecules gives lower energy. The thermodynamic equilibrium therefore favors the formation of o-H_2 pairs. It has been observed that the pair configuration can be achieved by keeping the crystal in a prolonged time.[23] This phenomenon, known as rotational diffusion, has been ascribed to quantum mechanical resonant conversion of an ortho-para to para-ortho pair by intermolecular magnetic dipole-dipole interaction. A rate constant of about 2 hours was predicted using this model, which is consistent with the experimental observations.

C. Solid Hydrogen as a Matrix Material

One of the most important considerations of matrix isolation spectroscopy is the choice of matrix material. Factors influencing the choice of dopant/host combination include: spectral compatibility, chemical reactivity, dopant isolation efficiency, and stringency of cryogenic requirements for achieving thermally stable low vapor pressure samples.[4] Common matrix materials such as rare gases and N_2 all share the common characteristics of being chemically inert, free of absorption spectra that would interfere with spectroscopic detection of the isolated species, rigid, and low vapor pressure. Argon and nitrogen are readily and cheaply available, being obtained in large quantities by the fractional distillation of liquid air. The other rare gases are more expensive, being present in the atmosphere only in very small amounts. Over the years, lots of spectroscopic studies of stable and unstable species using these matrix materials can be found in literature.

In most spectroscopic studies using rare gases and N_2 matrices, rotational structures were not resolved due to both homogeneous and inhomogeneous line broadening.[5] The rigidity of these matrix materials also increase the chances of trapping dopant molecules in the interstitial holes instead of lattice sites, resulting in amorphous structure and inhomogeneous broadening. For instance, ^{24} vibrational transition of CO in Kr and Xe matrices exhibits a typical width of 2 cm^{-1}. As will be discussed in Chapter IV, the corresponding spectrum is dramatically different in p-H_2 matrix from those mentioned above.

The absence of fine structures in vibrational bands limits our understanding of the detailed interactions and dynamics of molecules in condensed phases. In addition, the rigidity of these conventional matrices may limit the study of chemical reactions at cryogenic temperatures, as strong interactions from the surrounding matrix molecules may significantly distort reaction potential surfaces from those in the gas phase.[7,25] In particular the anisotropic interactions play important roles in reaction mechanism.

Solid H_2 has never been considered as a good matrix material until recently. As discussed above, the softness, low melting point, and high vapor pressure at cryogenic temperature of solid H_2 makes it difficult to prepare a sample of matrix with good optical quality. Nevertheless, high resolution spectroscopic work of solid H_2 in the later 1980s have demonstrated that optically transparent samples of more than 10 cm long can be prepared by depositing gas on a cold surface at about 7 K.[10] Together with the exceptionally narrow observed linewidth, solid p-H_2 has presented its potential as a matrix material for high resolution spectroscopy. The large lattice constant and the large amplitude of zero-point lattice vibration in solid hydrogen provide more free space for guest molecules than other matrices. For instance, the intermolecular distance in solid parahydrogen (3.79 Å) is considerably large than the interatomic distance in solid Ne (3.16 Å), as well as other rare gas solids, while the pair potential between H_2 molecules is similar to that between Ne atoms. Moreover, the large lattice constant of solid p-H_2 results in weak intermolecular interactions

between the dopant molecules and matrix molecules compared with those in rare gas matrices. Together with the large Debye frequency of lattice vibration of solid p-H_2, the lifetime of a guest molecule in excited states becomes much longer in p-H_2 matrix. This may be qualitatively ascribed to the origin of the sharp spectral linewidth observed in solid p-H_2. In some cases, the spectral linewidth is sharp enough to resolve not only *J* structure but also the *M* structure due to the orientation of the molecules in the anisotropic crystal field environment. The analysis of such fine structures promises rich information to shed light on understanding intermolecular interactions as well as molecular motion in the condensed phase.

The laser studies of o-H_2, HD and D_2 in p-H_2 crystals marked the first examples of ultrahigh resolution matrix spectroscopy in p-H_2.[26] These studies were followed by the work of CH_4,[23,27] where rotationally resolved lines with a typical width of ~300 MHz were observed and quantitatively analyzed. Since these promising results, attempts of studying a variety of stable and unstable molecules in p-H_2 have been carried out. To date, molecules such as CH_3F, CH_4 have been reported.[28] In addition, atomic species such as H (D, T), N, B, O, Xe, Kr, Al, Ag, Cu, Mg, Li in p-H_2 have also been studied.[12,21,29-31]

While the chemical inertness of rare gas matrices is unrivaled, it has been shown experimentally that unstable species also have extremely long life time in p-H_2 matrix. It has been observed that hydrogen cluster ions $H(H_2)_n^+$ have lifetime of days. The reactions of reactive species with H_2 molecules may be

endothermic or exhibit even a modest activation barrier. At cryogenic temperature, it is difficult to acquire sufficient energy to initiate the reactions. Studies of chemical reaction dynamics at low temperature in p-H_2 matrix have also been pursued.[32]

Chapter III. Experimental Apparatus

An experimental system consisting of a gas handling system, an inline ortho/para converter, and a sample cell housed in a liquid helium cryostat was designed and assembled for studying matrix isolation spectroscopy of solid hydrogen. A commercial Fourier transform spectrometer was used for recording the spectrum of the samples. The cryostat used for the experiment was modified from a commercial Dewar and a home-made copper sample cell fitted with a sapphire substrate was used. The details of these apparatus are discussed in this chapter.

A. Fourier Transformer Spectrometer

The working principle of a Fourier transform infrared spectrometer is based on the principle of Michelson interferometer. Using a Michelson interferometer as shown in Figure i, the incoming beam of a broad band radiation source is splitted into two equal components after the beam splitter. The component reaching moving mirror will have certain optical path difference x from the component reaching fixed mirror depending on the position of moving mirror. A power spectrum $f(x)$ as function of x can then be obtained by combining the two components again. This unique spectrum is known as the interferogram. The frequency spectrum can then be obtained by performing a Fourier transformation of the interferogram.

Figure i: Schematic diagram of Michelson Interferometer. Optical path difference is produced by moving of Moving mirror.

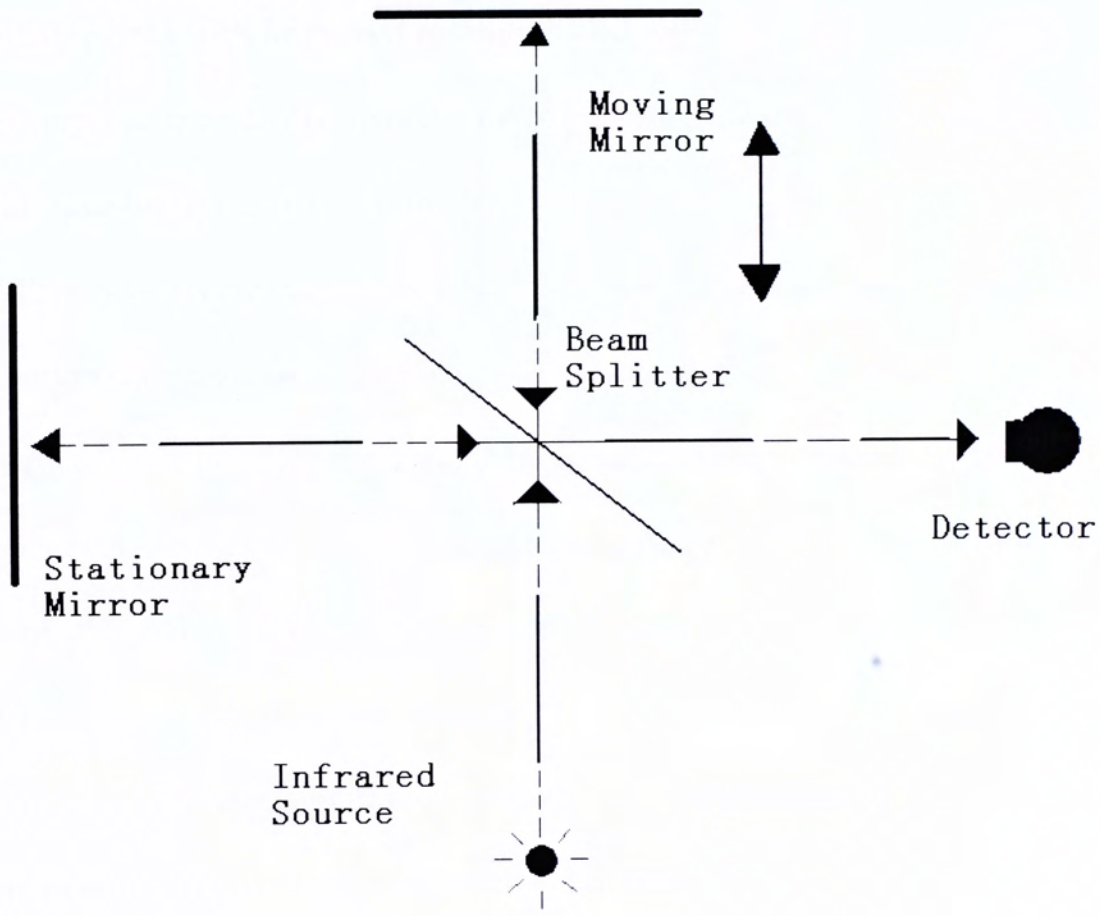

$$F(\frac{1}{\lambda}) = \int_{-\infty}^{\infty} f(x) e^{-i\frac{2\pi x}{\lambda}} dx \qquad (i)$$

While first introduced in 1911, the development of FTIR spectrometer has been greatly catalyzed since 1970s[33] by the advancement of computer technology. To date, the Fourier transformation can be completed in seconds using high speed computers. FTIR spectrometer has become common bench top instruments replacing the conventional dispersive spectrometers to produce rovibrational spectra with improved resolution and sensitivity in much shorter time. This improvement can be realized by considering the different detection schemes in these two types of spectrometers.

In a dispersive spectrometer, the power of a small frequency interval of a broad radiation source was selected using a small slit together with a dispersion device (such as a grating or a prism) and then measured by an infrared detector. The frequency spectrum is then obtained by putting together the power spectrum of all frequency intervals. This approach has a few drawbacks. First of all, the frequency selection greatly reduced the power reaching the detector, resulting in a much lower signal to noise ratio. The improvement of signal to noise ratio requires long data acquisition time. Secondly, the spectral resolution is determined by the width of the slit. A better resolution requires a narrower slit, resulting again a reduction of power reaching the detector. Since only a small spectral region was measured each time, the complete coverage of the radiation source will require much time to complete. The required time gets longer with better resolution.

These drawbacks are addressed in Fourier transform infrared spectroscopy. The resolution of an FTIR spectrum is determined by the maximum path difference between the two optical beams. In common practice, the resolution (σ) of an FTIR spectrometer can be estimated by the inverse of the optical path difference x. For instance, a spectral resolution of 0.1 cm^{-1} can be obtained by scanning the moving mirror for 1 cm, which can be completed in seconds. To date, spectrometers with a resolution of 0.001 cm^{-1} are commercially available.

The power of all frequencies emitted by the radiation source is measured by the detector simultaneously at all time. This multiplex principle results in better sensitivity, as first recognized by Fellgett, due to the fact that the actual measurement time for each frequency is the same as the measurement time of the whole spectrum for FTIR spectrometers whereas in dispersive spectrometers the actual measurement time for each frequency is much less than the measurement time of the whole spectrum. The gain in S/N using FTIR spectroscopy is $\sqrt{N}$, where N is number of spectral segments needed to cover the entire spectrum in conventional spectrometers. In addition, the simultaneous measurement of all frequencies in FTIR spectroscopy gives rise to a much higher optical throughput (known as the Jacquinot Advantage) and thus lower noise level compared to dispersive spectrometers. The fast speed in FTIR spectroscopy makes it possible to apply signal averaging technique. Since the scanning speed of the moving mirror is determined by the response of the detector, with an appropriate detector, spectra with good signal to noise ratio

can be obtained by fast scanning and signal averaging (so-called coaddition) of a number of spectra in a short time. The improvement in S/N using signal averaging is $\sqrt{n}$, where n is the number of spectra used for averaging. Since the resolution is not limited by the input aperture of the interferometer, the power level reaching the detector can be increased appreciably by choosing the appropriate aperture size. This again contributes to a better S/N in the spectra.

The fast acquisition of spectra in FTIR spectroscopy is easily realized. The multiplex principle allows the detection for the entire spectral region at all time, which significantly shortens the time of acquiring data with good S/N. As discussed above, the improvement in sensitivity requires much less time in recording a spectrum to the desired S/N. The fast scanning mechanism in obtaining the interferogram also contributes the speed accomplished by FTIR spectroscopy.

In addition, FTIR spectrometer provides much better absolute frequency calibration. By employing a frequency-stabilized He-Ne laser as an internal standard to determine accurately the optical path difference x, accurate frequency calibration can be obtained after the Fourier transformation. This characteristic is known as the Connes Advantage. It is worth to note that the resolution of the resultant frequency spectrum has little effect on the absolute frequency calibration.

In practice, there are many technical concerns in building an FTIR spectrometer. For instance, apodization is a mathematical procedure to

minimize the fringes appearing at the wings of spectral transitions due to the finite optical path difference in the interferogram, the choice of the apodization function may affect the effective resolution, lineshape, and linewidth. Other considerations include phase correction, numerical filtering, analog to digital sampling, *etc*. Readers are referred to a number of excellent reviews for the details.[33]

The FTIR spectrometer used for this experiment was a Bruker Vertex 70 model, composed of a Michelson interferometer, an electronic control system to couple the interferometer and the PC, which is used for performing the Fourier transformation. The frequency coverage of our spectrometer ranges from 400 to 25000 cm^{-1} with the combination of a globar and a tungsten lamps, a KBr and a quartz beam splitter, and a DTGS and a silicon photodiode detectors. The highest unapodized resolution is 0.16 cm^{-1}. In addition to usual data acquisition mode, our spectrometer is also equipped for time-resolved spectroscopy with step scan at a data acquisition rate of 200 MHz and rapid scan to obtain 60 spectra per second at a resolution of 16 cm^{-1}. In our studies, the size of our cryostat is too great to fit into the sample compartment. We therefore sent the light beam out to our sample and used an external InSb detector for the detection. A schematic diagram of the optical layout of our experiments is given in Figure ii. Most spectra reported in this thesis were recorded at 0.2 cm^{-1} resolution with 2000 coadditions using a KBr beamsplitter, a globar source, and the liquid-N_2 cooled InSb detector. No improvement in the signal to noise ratio

Figure ii: Schematic diagram of the optical layout of our experiments. The front port was used for passage of the detecting light. The light was focused to pass through the sample cell and collected by the external InSb detector.

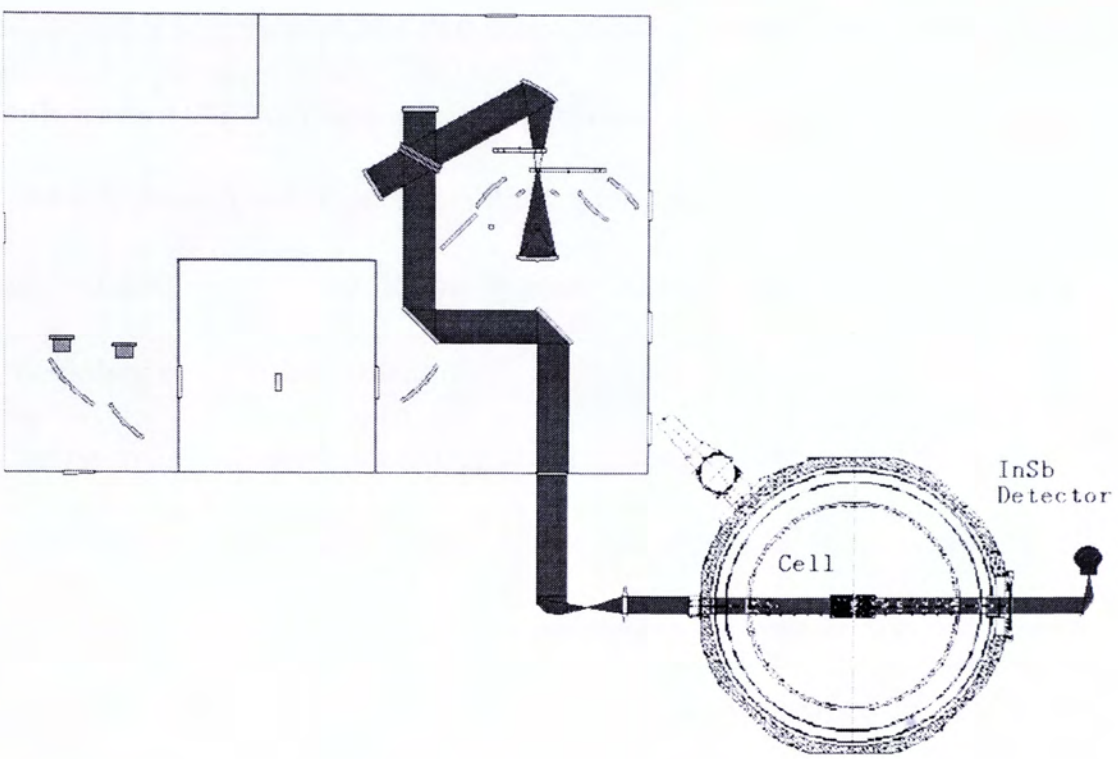

was observed with coaddition more than 2000 times.

B. Cryostat and Sample Cell

The cryostat used for this experiment was a modified version of the commercial HDL-8 Dewar from Infrared Laboratories, as shown in Figure iii. The helium Dewar is composed of two cryogenic vessels. The Liquid N_2 vessel directly cooled a radiation shield that surrounds the Liquid He vessel and the cold work surface. All the interior Dewar surfaces were covered with aluminum foil in order to provide additional shielding. Along the optical axis of the Dewar, two CaF_2 windows of 1 inch in diameter were installed and sealed by o-ring to allow the passage of infrared radiation.

A home-made copper sample cell of 3 cm long was installed on the cold plate of the Dewar to maintain at or close to 4.2 K when Liquid He was filled in the can. A bore of about 1.5 cm inner diameter was cleared for the passage of light and sealed with a pair of sapphire windows using indium gaskets. The gas inlet was made of a stainless steel tube of 0.06 inch in diameter soldered on the top of the cell extending to the gas handling system outside the Dewar. This cell was originally designed for growing large p-H_2 crystals. It is however, applicable for matrix isolation spectroscopy without modification since a thin film of crystal can be formed uniformly outside the cell by slowly flowing gas on to the sapphire surface. For this purpose, a vacuum feedthrough for a stainless steel nozzle modified from a syringe needle was used to deliver the

Figure iii : The liquid helium Dewar for the preparation of solid hydrogen. The sample cell with sapphire window substrate is screwed on the cold plate of the helium can. The optical beam is irradiated along the optical axis of the Dewar for FTIR spectroscopy.

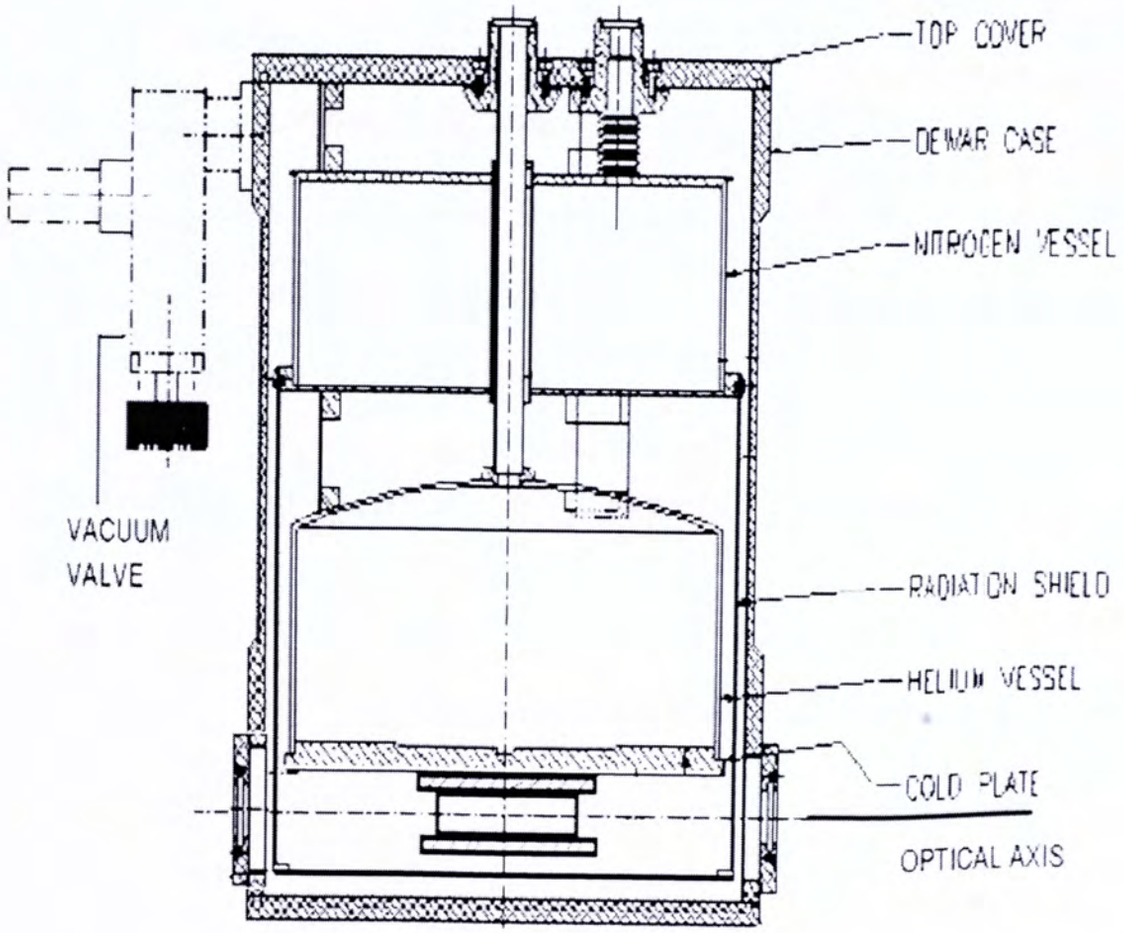

gas from the gas line to the cell. The nozzle was placed at a distance of 1~1.5 cm from the sapphire window. It was found from the recorded spectra that the optimized distance was about 1.5 cm. At this distance, the deposition appeared to produce a sample of uniform length with reproducible optical quality.

Two silicon diode temperature sensors from Lakeshore Cryotronics, (DT670-SD) were used to monitor the temperatures of the cold plate and the sample cell, respectively. It was found that both sensors displayed almost identical temperature even during the deposition process suggesting heat transfer was sufficient in our system. Since there was no temperature control in our Dewar, we controlled the temperature of the deposition by controlling the rate of gas flow during the deposition process.

C. Gas Handling System and Ortho-para Converter

The complete gas handling system for preparing solid hydrogen is shown in Figure iv. An inline ortho/para converter was used to convert normal H_2 gas to p-H_2 gas. A stainless steel vessel was used to premix the dopant molecules with p-H_2 for the growth of matrix-isolated samples.

The use of p-H_2 is essential in reducing the intermolecular interactions and spectral widths of the matrix-isolated sample. The conversion from normal H_2 (with an ortho/para ratio of 3 to 1) to p-H_2 cannot be achieved simply by lowering the temperatures without the presence of an inhomogeneous magnetic field in the range of 14 to 21 K, the self conversion rate between of o- and p-H_2

Figure iv: Gas line system for the experiment. para-H_2 coming out of the converter rushed into the storage chamber to mix with CO impurity molecules. After that, mixture gas deposited on the surface of substrate in the cryostat cell to form thin film for study of spectroscopy. ⊗ denotes the vacuum valve used in experiments.

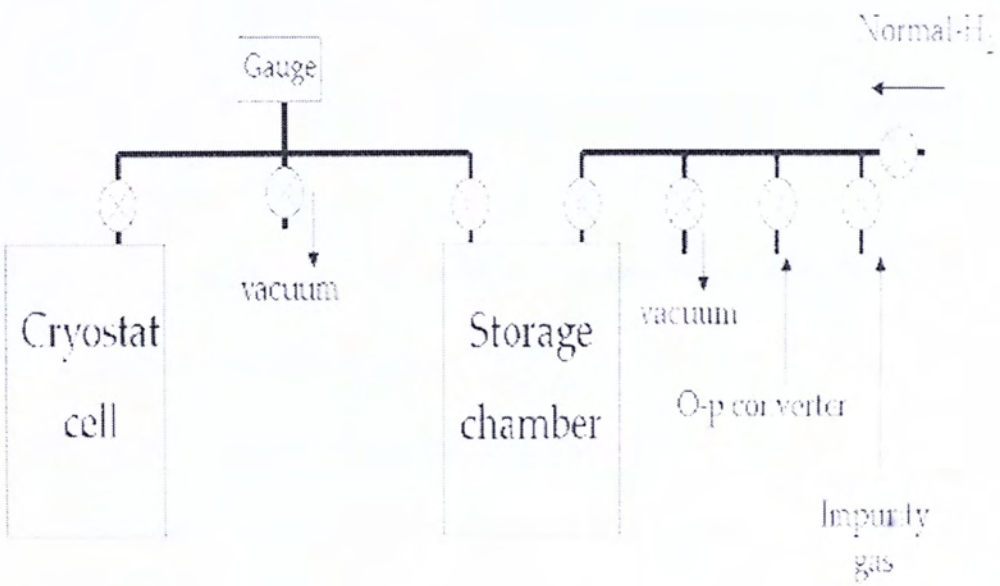

mixture via collision mechanism exhibits a rate constant of 5.3×10^{-6} sec^{-1}, requiring several weeks to obtain an equilibrium mixture of ~99% p-H_2.[8] Physical methods, *e.g.* cryogenic distillation, are inapplicable for separating ortho and para species because their physical properties are almost identical.

This ortho/para conversion rate can be greatly increased by using a suitable catalyst that provides an external inhomogeneous magnetic field around the absorbed hydrogen molecules so that fast equilibrium between the o-H_2 and p-H_2 concentrations can be achieved by lowering the temperature of the catalyst. Based on this approach, ortho/para converters consisting paramagnetic ferric oxide (Fe_2O_3) from C*CHEM as the catalyst were built for the production of p-H_2 from normal gas.

Two designs of ortho/para converters (Figure v) have been built. The first one was designed by Sibener and coworkers[34] for using liquid H_2 as coolant. As shown in the figure, normal H_2 gas diffuses through the catalysts to the bottom before it is released. Since the temperature of the converter is equilibrated at ~20K with liquid H_2, the effective conversion temperature is 20K to generate ~99.8% para-enriched H_2. Unfortunately, the usage of liquid hydrogen coolant is not available in Hong Kong. Attempts at controlling the temperature of this converter using cold He vapor was not successful. We therefore designed a simpler version of converter as shown in the bottom of Figure v. It was composed mainly of a 40 cm long stainless steel tube to house the catalyst. Two valves were installed at the top of the converter. A plug valve was used to

Figure v: Schematic diagram of two designs of ortho/para converter. The bottom one was used in our experiment.

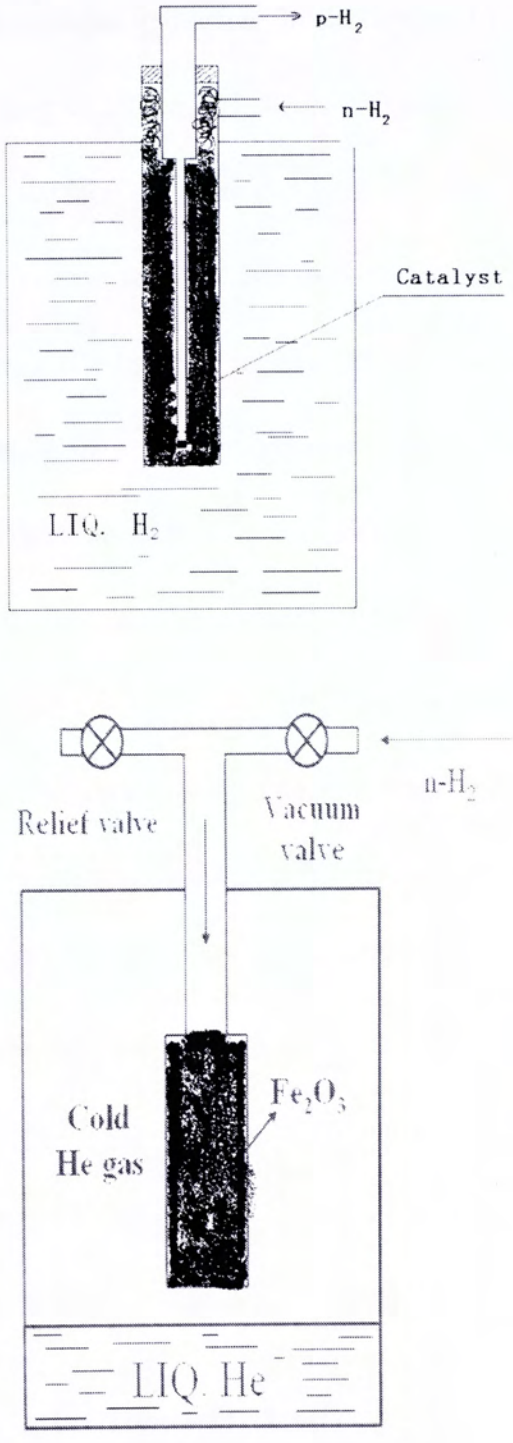

control the normal H_2 flowing into the converter as well as the para-enriched H_2 flowing out to the gas storage vessel. The other one was a relief valve for pressure release in case of a sudden pressure build up in the converter. The catalyst was activated by heating at 150 to 175 ℃ for a few hours to remove gas molecules absorbed on the surface of the catalyst. In the operation, after absorbing normal H_2 gas, the converter was isolated and kept in the liquid He can of the cryostat dewar above the liquid He level, thus it could be cooled by the cold He gas to low temperature required for conversion. Temperature was adjusted by changing the separation between the bottom of the converter and the liquid He level. When the para-enriched hydrogen was needed for experiment, the converter was lifted as quickly as possible to release the gas to the storage vessel. The para-enrichment using this approach is about 99%.

Since the volume of the converter is limited by the size of the neck-tube of our helium Dewar, its capacity is too small to have stable flow of p-H_2 gas. Another problem of the converter is the great temperature gradient along the stainless tube. A new helium Dewar has been designed and purchased to accommodate ortho/para converter of large volume with smaller temperature gradient so that higher para-enrichment can be achieved.

D. Determination of o-H_2 Concentration

The infrared spectrum of solid hydrogen varies dramatically with different ortho/para ratio. As shown in Figure vi, the rovibrational spectrum in the 4100

Figure vi: The comparison of the IR fundamental absorption spectra which contains 99% para H_2 and 50% para H_2 respectively. The absorption of $Q_1(0)$ and $Q_1(0) + S_0(1)$ bands changes dramatically with decreasing the ortho H_2 concentration.

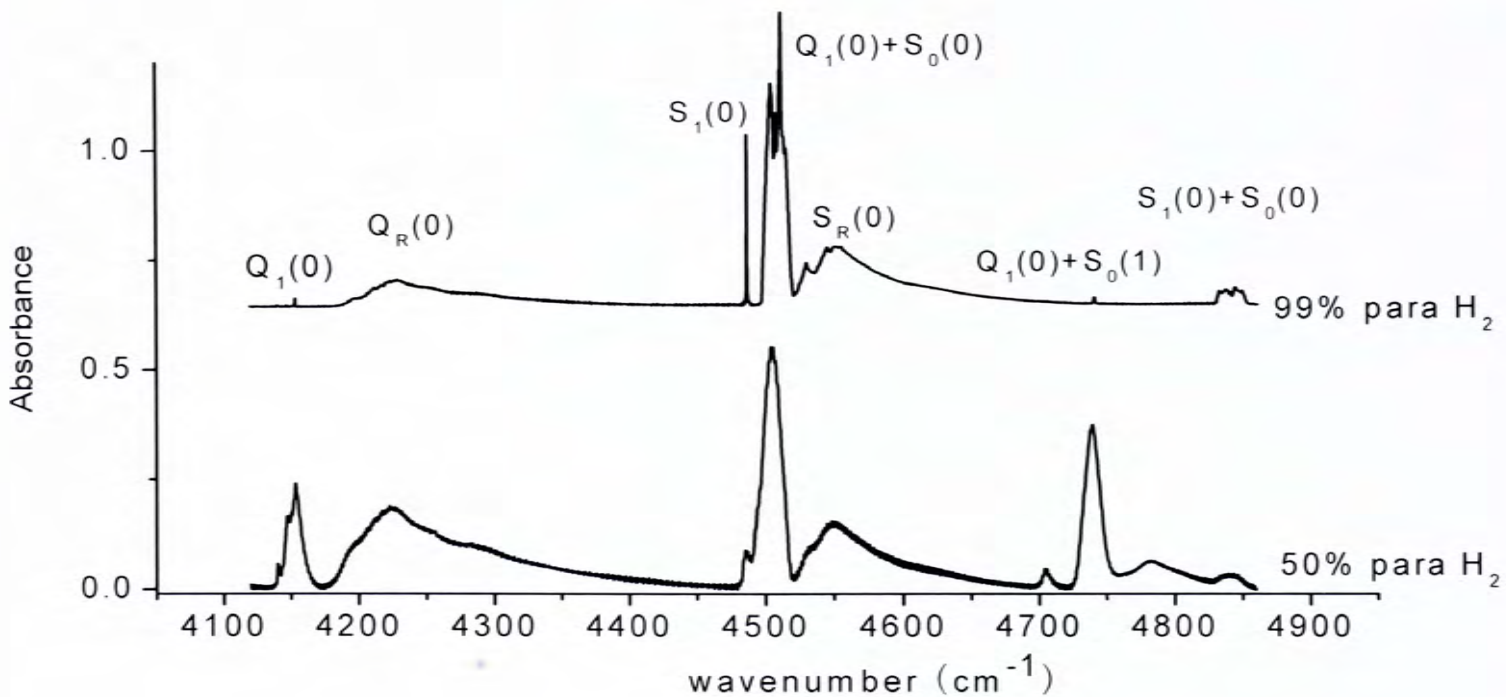

-4900 cm^{-1} region is greatly simplified by lowering the ortho concentration. The detailed assignment and theory of the spectrum are well document and readily found in literature.[35] One of the most interesting phenomena in the spectrum with increasing o-H_2 concentration is that the drastic increase of intensity of $Q_1(0)$ transition, in addition to the increasing spectral widths. It has been pointed out that the $Q_1(0)$ transition is strictly forbidden in the absence of o-H_2. The intensity of $Q_1(0)$ can serve to indicate the o-H_2 concentration. As we show below, one can determine the o-H_2 concentration as well as optical length of the matrix sample by quantitatively analyzing of the spectral pattern.

According to Gush *et al.*, the dependence of $Q_1(0)$ band integrated intensity on the ortho H_2 and para H_2 fractions is given by:[36]

$$(1/l(cm))\int \log_{10}(I_0/I)d\tilde{\upsilon}(cm^{-1}) = aF_o^2 + bF_oF_p = bF_o + (a-b)F_o^2 \qquad \text{(ii)}$$

where l is the thickness of the sample and F_o and F_p denote the mole fraction of o-H_2 and p-H_2 respectively, in the sample. The constants a and b, with empirical values of 45 cm^{-2} and 30 cm^{-2}, are related to the transition probabilities. In the limit of low o-H_2 concentration, the $Q_1(0)$ band intensity is directly proportional to the ortho H_2 concentration. In other words, F_o can be determined from Eq.

(ii) if the thickness of the sample is known. To estimate the length of the sample, we used the approach of Tam and Fajardo.[37] According to the Beer-Lambert's law, the integrated absorbance of a transition is proportional to the length of optical path. By plotting the integrated absorbance of the $Q_1(0)$+$S_0(0)$ line against the thickness of p-H_2 samples, they obtained an

empirical relationship:

$$l(cm) = \int \log_{10}(I_0 / I) d\tilde{\upsilon}(cm^{-1}) / 82(cm^{-2}) \qquad \text{(iii)}$$

Applying these equations to our observed spectra, the typical thickness and o-H_2 concentration in our para-enriched matrix samples were determined to be 2 mm and 0.4%, respectively.

E. Preparation of Matrix-isolated Species

Samples of matrix isolated species were grown from pre-mixed gas, which was prepared and stored in a stainless steel vessel. In a normal run, certain amount of species of interest was stored in the vessel prior to the addition of para-enriched H_2 gas from the converter. In order to have well-separated dopant molecules in the para-H_2 matrix, the typical dopant/para-H_2 ratio is about 10^{-5} to 10^{-6}. In growing the solid sample, the mixture gas was flowing at a rate of 3.6×10^{-6} mol per second to deposit on the cold sapphire surface of the sample cell. At this flow rate, the temperature of the substrate was about 5K, slightly higher than the liquid He temperature of 4.2 K. The low growth temperature is more desirable since the difference of melting points between the dopant and p-H_2 molecules is so great that high deposition temperature tends to produce large clusters of dopant molecules, resulting in samples with low optical transparency. Dopant molecules deposited on the substrate is expected to have no further diffusion at this low temperature. Because of the excellent thermal conductivity of solid hydrogen, the sapphire window and the

OFHC (Oxygen Free High Conductivity) copper, the temperature was maintained steadily throughout the deposition process of about 1.5 hour. Samples prepared this way were optically clear suggesting little strain in the solid. This was also confirmed by the observed linewidths in the infrared spectrum.

Chapter IV. Spectroscopic studies of CO in solid hydrogen

A. Matrix Isolation Spectroscopy of CO: a brief overview

While being one of the simple diatomic molecules, CO presents a system of academic interests. Because of the back donation of electrons from the oxygen atom to form a dative bond, properties of CO cannot be predicated by simple bonding theory. For instance, CO has very small dipole moment with the negative end located at the C atom. The melting and boiling points of CO are much lower than other heteronuclear diatomic molecules. These properties make it an excellent system for high-level theoretical studies. Molecules of CO in rare gas matrix form one of the simplest systems for matrix isolation spectroscopy. Nevertheless, only the system of CO in Ar matrix has been extensively studied.[6] Studies of CO in Kr and Xe matrices were only reported a few years ago. The very low melting point (68 K) CO compared to rare gas matrix materials makes it difficulty to anneal the sample for the removal of matrix defects. This difficulty, however, is not present in the case of p-H_2 matrix. It has been known that crystals of H_2 can be grown from flowing gas onto a cold surface below ~7K. Nevertheless, spectroscopic studies of CO in p-H_2 have yet to be reported.

Spectroscopic studies of molecules in p-H_2 matrix have shown that small

molecules, such as D_2, HD, CH_4,[10,27] can have nearly free vibrational and rotational motions while large molecules such as CH_3F and CO_2 only exhibit hindered vibrational motion without rotational motion.[28] This may be ascribed to the size effect and stronger intermolecular interactions in the latter case. In the case of CO, its size (r~1.62 Å) is much smaller compared to the intermolecular separation of 3.79 Å in solid p-H_2. It is expected CO occupying a lattice site will not introduce server crystal distortion. The small dipole moment as well as higher order moments introduces only very weak intermolecular interactions to hinder the vibration and rotation of CO in p-H_2 matrix. Comparing the infrared spectra of CO in p-H_2 to those of the rare gas matrices may provide a better understanding of structures, motion, and relaxation of molecules trapped in these matrices.

B. Observation and Preliminary Analysis

i. CO in Normal H_2 Matrix

The spectrum of CO in normal H_2 matrix was carried out as a preliminary study. Figure vii shows the spectrum around the fundamental band of CO at different concentrations recorded at a resolution of 0.2 cm^{-1}. A single peak at about 2140.81 cm^{-1} was observed at CO concentration of 0.5 and 5 ppm. Comparing the fundamental frequency of CO at 2142.37 cm^{-1} in the gas phase, the peak was assigned as the pure vibrational transition of CO. The shift

Figure vii: IR absorption of CO trapped in normal hydrogen matrix. Spectra of 0.5ppm, 5ppm and 50ppm CO are presented respectively. Relative low concentrations of CO exhibit only one peak at 2140.81 cm^{-1} while 50ppm concentration gives us one main peak, slightly redshifted to 2140.54 cm^{-1}, with a satellite peak at about 2141.42 cm^{-1}. The profile of the 50ppm situation is not shown completely because of saturation of absorption. The spectrum resolution is 0.2 cm^{-1}.

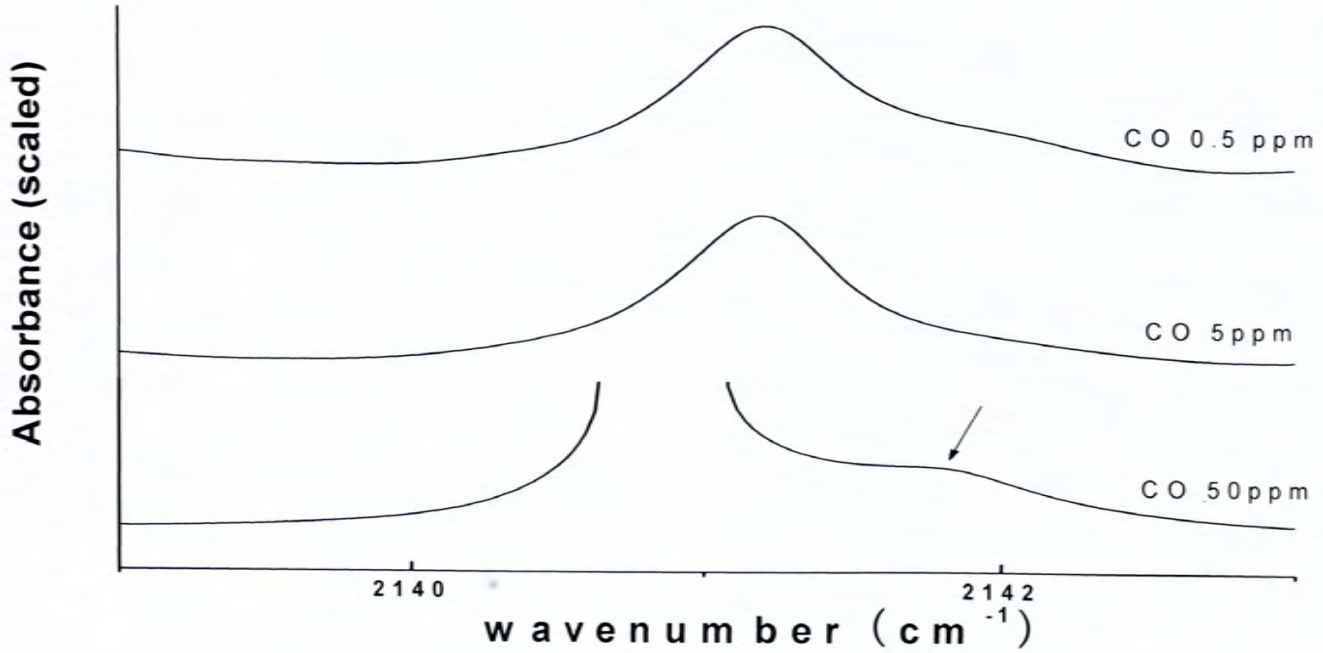

of -1.99 cm^{-1} was much smaller than those observed in rare gas matrices.[24] This is expected from the weak intermolecular interactions in the system.

As the CO concentration was increased, the main peak shifted further down in frequency. At 50 ppm of CO, a shift of -1.83 cm^{-1} was observed. The greater shift may be ascribed to the stronger interactions at higher CO concentrations while a quantitative argument has yet to be established. It can be seen from Figure vii that a small shoulder appears at 2141.42 cm^{-1}. This observation may reflect that the concentration of CO is high enough to cause significant defects in the crystal or formation of dimers and other clusters. In addition, a weak feature at 2151.49 cm^{-1} was observed. While the nature of this peak is yet to understand, it appeared to grow with increasing CO concentration. This observation suggests that it may be due to CO molecules. To simplify the spectrum for further studies, we therefore restricted the CO concentration to below 20 ppm.

The absence of rotational structure suggested that strong intermolecular interactions prevent CO from rotating. The reduction of o-H_2 concentration was necessary to allow the rotation of CO.

ii.CO in Hydrogen Matrix of 50/50 Mixture

By proper mixing the 99% para-enriched H_2 gas and normal H_2 gas, 50% para-enriched H_2 was obtained. Figure viii shows a spectrum of 10 ppm of CO in a H_2 matrix with 50/50 ortho para mixture. The overall appearance

Figure viii: IR absorption spectra of 10 ppm CO in 50% para H_2 matrix. No fine structures other than the vibration profile were detected, similar to the normal H_2 case. A weak peak appeared at 2151.49 cm^{-1}.

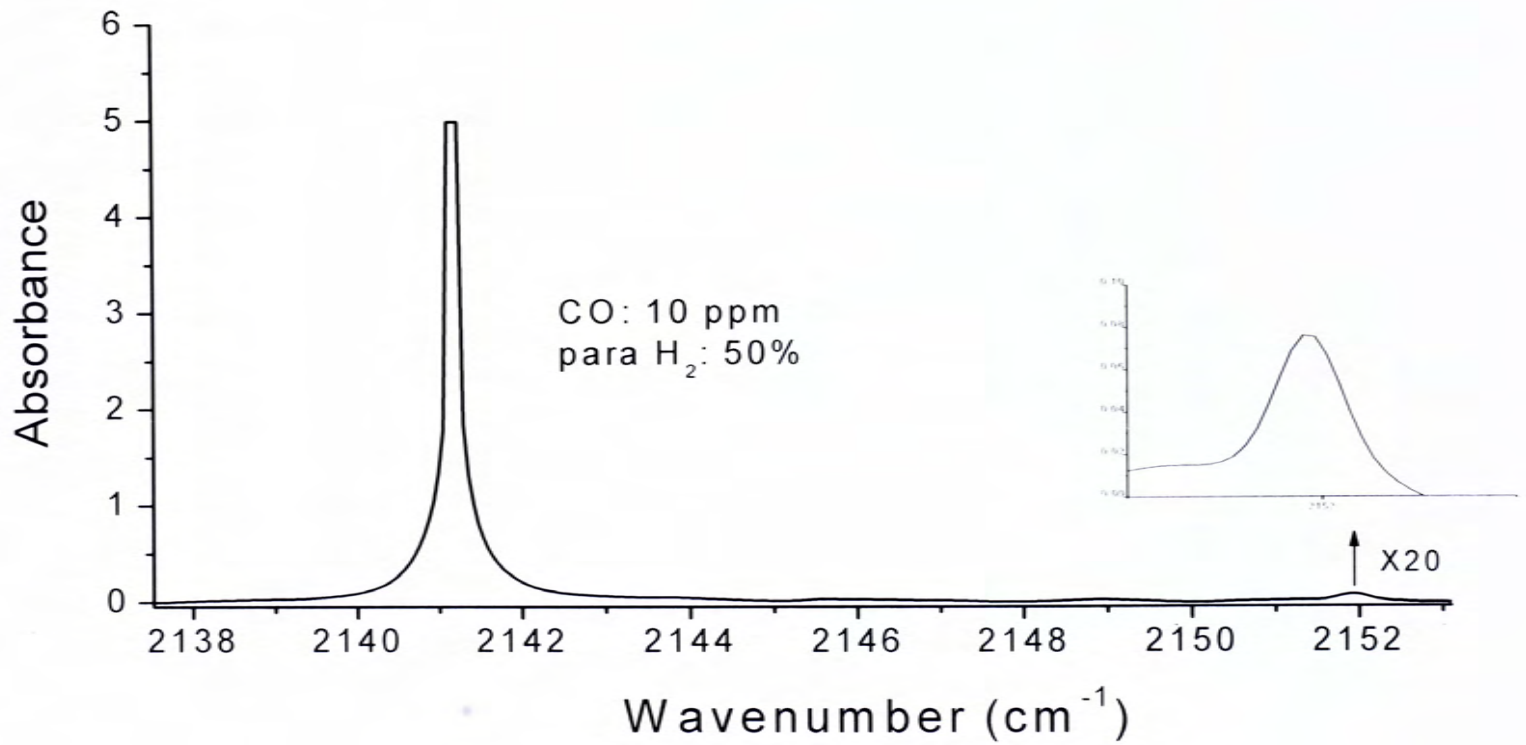

was similar to the case of normal H_2. A single peak was observed at 2140.75 cm^{-1} with a weak feature at 2151.49 cm^{-1}, suggesting that the reduction o-H_2 was not sufficient to allow CO to rotate. On the other hand, the shoulder peak observed in 50 ppm normal H_2 matrix was not observed in this case. The absence of rotational structure led us to further reduce the o-H_2 content in the matrix.

iii. CO in Para-enriched Solid Matrix

The dramatic effect of o-H_2 content on the spectrum was observed by using highly para-enriched H_2 matrix. Figure ix shows a spectrum of 5 ppm of CO in 99.4% p-H_2 matrix. In contrast to the cases discussed above, four groups of lines denoted as A, B, C and D were observed in Figure ix. Each group appeared to be composed of features not completely resolved. The most prominent line in each group were located at 2137.45 cm^{-1}, 2140.49 cm^{-1}, 2142.83 cm^{-1} and 2145.78 cm^{-1} respectively, almost with the same spacing of 3 cm^{-1}. The observed linewidth for these lines were about 0.3 cm^{-1}, which appeared to be limited by the apodized resolution of our spectrometer. In order to understand the nature of the lines, we studied the spectral pattern at different degree of para-enrichment as shown in Figure x. It is seen in trace (d) that the spectral pattern for 3.6% ortho was similar to that of normal H_2, suggesting rotation of CO was quenched. However, as the o-H_2 content was reduced to 1.4% (trace c), the groups of lines appeared. By further reducing the o-H_2 content, it was found that the four prominent lines mentioned above remained almost unchanged in

Figure ix: IR spectrum of 5 ppm CO in 99.4% para H_2 matrix. Four main peaks with shoulder peaks appeared when the orhto H_2 concentration fell to 0.6%. The band were assigned to be other rotation motions of CO, or the CO(ortho-H_2)n clusters features. However, the latter was ruled out by changing the ortho-H_2 concentration which will be discussed in following.

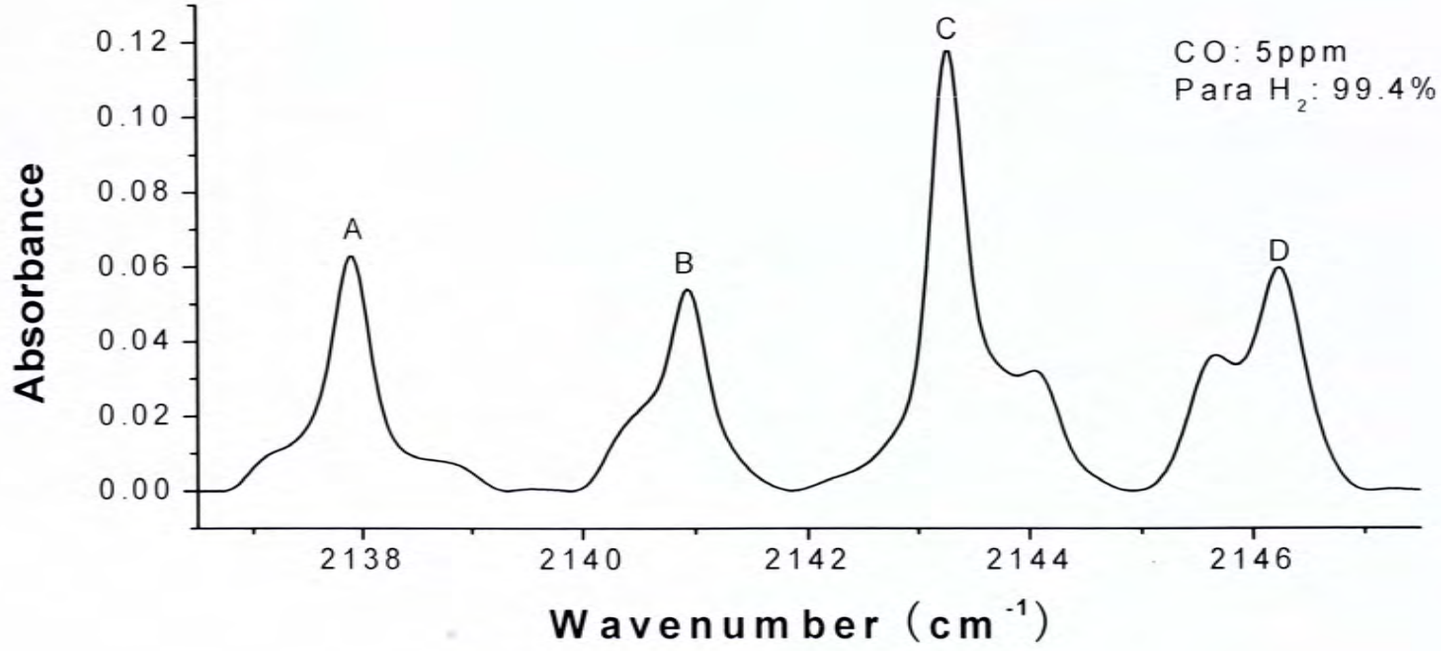

Figure x: Comparison of profiles of CO in different ortho H_2 concentration samples. In curves a, b, and c, relative low concentration of ortho H_2, the profiles almost remain the same except that some ratios of the peaks change. In curve d, one single broaden peak is detectable which is consistent with the case in the normal H_2. The concentration of CO was 5 ppm for all the spectra below.

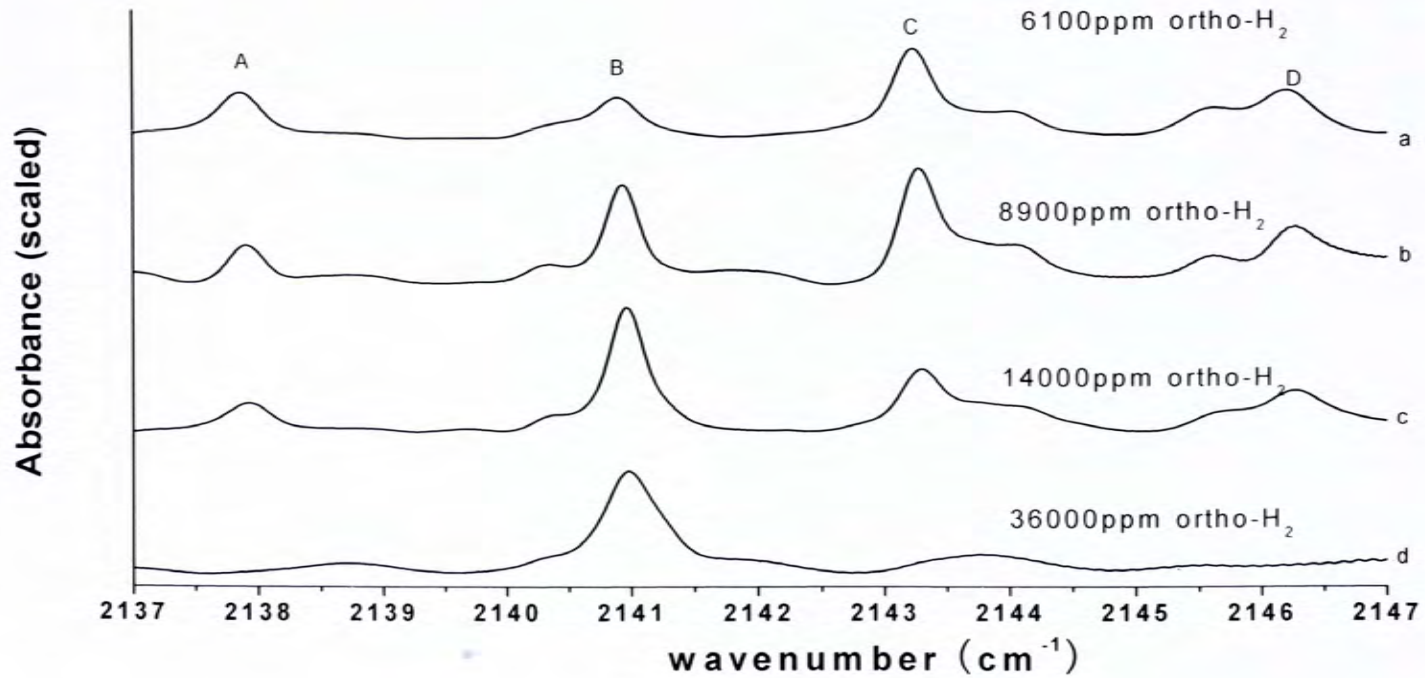

relative intensity with an exception of the line in group B, which decreased with reducing o-H_2 content. In addition, the line width as well as the transition frequencies also remained unchanged.

These observations led us to tentatively interpret the four prominent lines to the rotational structure of CO. It is known that the $\Delta J = 0$ transition is strictly forbidden for isolated gaseous CO molecule. In solid H_2, however, the presence of a neighboring o-H_2 molecule can induce a pure vibrational transition together with an orientational change of the o-H_2 molecule through the quadrupole induce dipole mechanism. It is the same mechanism responsible for the $Q_1(0)$ transition of p-H_2 molecules in the presence of o-H_2. Similar to the $Q_1(0)$ line of p-H_2, the intensity of $\Delta J = 0$ transition of CO is expected to reduce with lower o-H_2 content in the matrix. Based on this argument, the line at 2140.49 cm^{-1}, which was weaker with reducing o-H_2, was assigned to Q branch of the CO. This assignment is also consistent with the assignment of the pure vibrational transition at 2140.75 cm^{-1} in samples with high o-H_2 content. Once the position of Q branch was determined, the remaining lines were assigned to P(1) at 2137.45 cm^{-1}, R(0) at 2142.83 cm^{-1}, and R(1) at 2145.78 cm^{-1}, respectively. The complete assignment was listed in Table II.

Because of the anisotropic crystal environment, each J transition is expected to further split due to M states. The intensities for the M transitions depend on the polarization of light source. For polarization parallel to the crystal Z axis, only transition with $\Delta M = 0$ is allowed whereas for polarization perpendicular

Table II: Observed frequencies, and tentative assignments of the fundamental bands of CO in solid para H_2.

Observed frequencies (cm^{-1})	Tentative Assignments
2137.45	P(1)
2140.75	Q(0)
2142.83	R(0)
2145.78	R(1)

to the crystal Z axis, only transitions with $\Delta M = \pm 1$ are allowed. Since there is no documented information for the magnitude of the M splitting, it is possible that the partially resolved satellite peaks in each group were due to the M splitting. The polarization dependence of the peak intensity was therefore studied. However, there was no obvious polarization dependence on the relative intensity of all the lines as well as the appearance of the overall spectrum. This observation leads to two possibilities: (1) the satellite peaks were not due to M splitting and (2) the M splitting may not be resolved because of the broad observed linewidth of 0.3 cm^{-1}. The second point was also consistent with the slight irregularity of spacing between the rotational lines.

In order to investigate the nature of the satellite peaks, the effect of CO concentration on the spectrum was studied. As shown in Figure xi, the intensities of the satellite peaks increases with increasing CO content suggesting they may be due to dimers or higher clusters of CO or dimers of CO and o-H_2. Considering the low concentration of CO and o-H_2 molecules in the sample, the probability of forming dimers from these molecules is very low. As a result, these satellite peaks were much weaker than the main features. Nevertheless, there is no clear evidence in Figure xi to support either case. If these satellite peaks are indeed due to dimers or clusters, it will imply that CO in these systems decouples its rotation from the dimers. As a result, rotational structure similar to that of matrix isolated CO appears as satellite peaks around the prominent lines. This situation is quite different from the case of gaseous dimer

Figure xi: Spectra of different CO concentrations. The side peaks increases with increasing CO content.

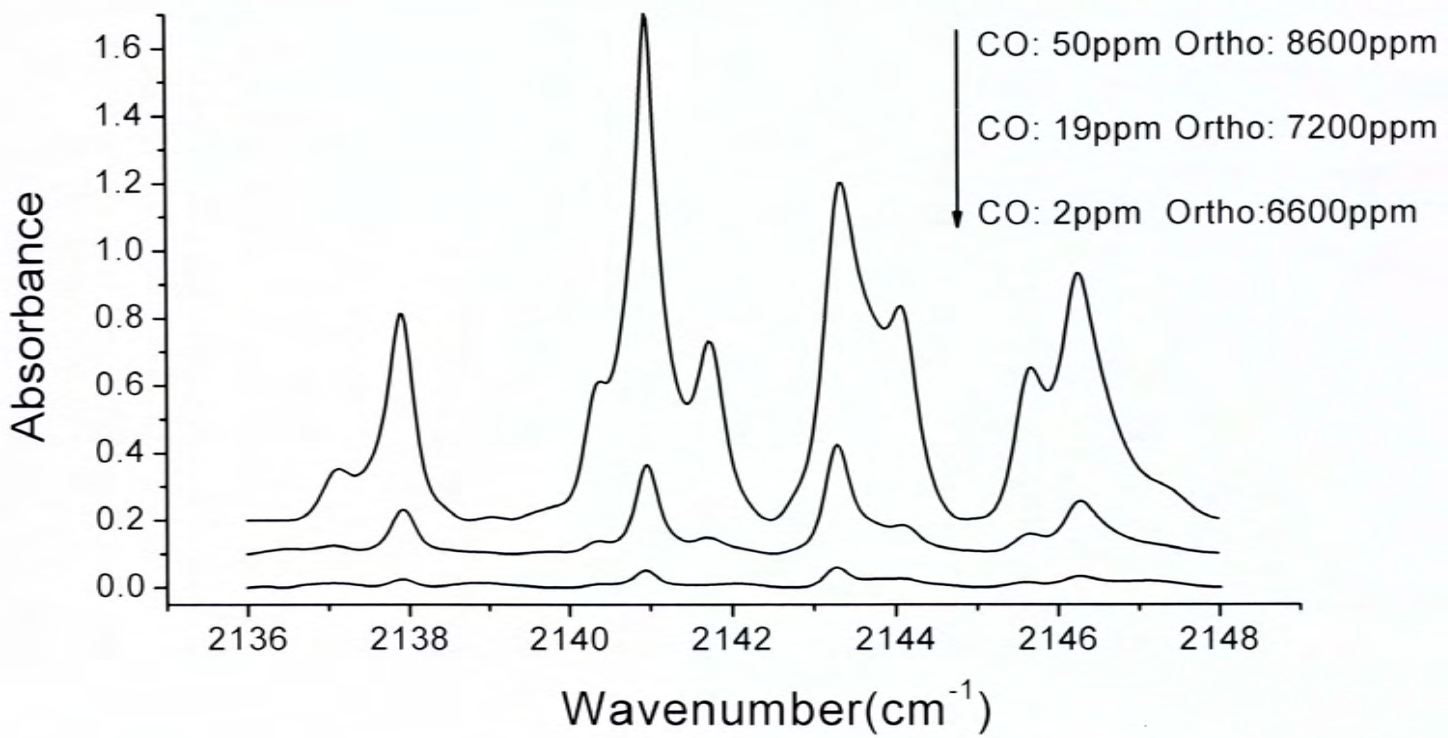

molecules, where the rotation of individual molecules is coupled to give an overall rotation.

The time dependence of the spectrum was also studied. By standing the sample at 4.8 K for 48 hours, we found no observable change of the spectrum indicating that either equilibrium of the system was established at the same time of matrix formation or the temperature was too low for diffusion of CO molecules in the matrix. Because of the high vapor pressure of both CO and H_2 molecules, no attempts were made to anneal the matrix sample at elevated temperature.

C. Discussion

Our study to date has provided a self consistent, yet qualitative picture to account for the main features of the rovibrational spectrum of CO in p-H_2. Nevertheless, there are some weaker features yet to be assigned, for instance, the nature of the transition at 2152 cm^{-1}. More extensive and systematic work is needed for a better understanding of the spectrum.

The infrared spectrum of CO in p-H_2 crystals is more complex than expected. The effect of o-H_2 content in the sample greatly changes the appearance of the spectral pattern. The quantitative model to account for the effect of o-H_2 content on the spectrum is yet to explore. This work no doubt provides the experimental information for this pursuit.

In the present work, the p-H_2 matrix used contained ~0.6% of o-H_2. This is

limited by the present apparatus. It is more desirable to use matrix with para-enrichment more than 99.99%. A further simplification of the spectrum is expected under this condition. A new ortho/para converter and a new liquid helium Dewar have been designed and purchased for the purpose. With this new apparatus, the control of ortho/para ratio in the matrices will be greatly improved.

The typical observed linewidth of 0.3 cm^{-1} appears to be limited by the resolution of our FTIR spectrometer. The absence of polarization dependence on the relative intensity suggests that *M* splitting is buried in the linewidth. It will be interesting to investigate the spectrum at a better resolution in order to clarify this point. One of the choices is to use high resolution laser spectroscopy such as difference frequency laser spectroscopy. Work along this line is underway.

Chapter V. Concluding Remarks

This work, while not complete to date, has demonstrated that rotational motion of CO is present in para-enriched solid H_2 matrices as a result of the small size of CO as well as weak intermolecular interactions. As the content of o-H_2 is increase, the strong intermolecular interactions between o-H_2 and CO quench its rotation. This leaves CO vibrating at the lattice sites. As shown in the spectra, a single vibrational transition is observed once the rotation is quenched. The critical concentration of ortho H_2 for quenching the rotation of CO is about 97%. Theoretical model to quantitative predict the critical o-H_2 concentration is yet to explore.

Part of our future work should focus on improving the present experimental conditions, as discussed in the previous chapters. With these improvements, it is hoped to provide better experimental data, which in turn leads to a general understanding of the physical picture of motions of molecules embedded in p-H_2 matrix.

Spectroscopy of solid hydrogen has provided a load of possibilities. Many experiments related to this work can be pursued using the apparatus built in the past few years. Some interesting subjects include the relaxation process of molecules in p-H_2, diffusion of molecules in p-H_2 matrix, and the effect dopant molecules on the spectrum of H_2 itself. The relaxation process is related to the observed linewidth, for which a general theory has yet to be developed. The

diffusion of molecules in p-H_2 is related to the formation of clusters of dopants in p-H_2 sample. The effect of dopant molecules on the spectra of H_2 provides information in understanding the intermolecular potential. A variety of techniques can be applied for these studies including Raman spectroscopy, time-resolve spectroscopy, double resonance, electric-field induced infrared spectroscopy, *etc.* In addition, study of reaction dynamics in p-H_2 matrix has been pursed by a number of groups. Interesting results have also been reported.

Reference

(1) Lewis, G. N.; Lipkin, D.; Magel, T. T. *Journal of American Chemistry Society* **1941**, *63*, 3005.

(2) Ogawara, Y.; Bruncau, A.; Kimura, T. *Analytical Chemistry* **1994**, *66*, 4354.

(3) M. L. Klein and J. A. Venables *Rare Gas Solids* **1977**, London ; New York : Academic Press

(4) Cradock, S. *Matrix Isolation* **1975**, Cambridge ; New York : Cambridge University Press

(5) Hollas, J. M. *Modern Spectroscopy* **1996**, Chichester ; New York : J. Wiley

(6) Dubost, H. *Chemical Physics* **1976**, *12*, 139.

(7) Silvera, I. F. *Review of Scientific Instruments* **1980**, *52*, 393.

(8) Van Kranendonk, J. *Solid Hydrogen* **1983**, New York : Plenum Press

(9) Okumura, M.; Chan, M.-C.; Oka, T. *Physical Review Letters* **1989**, *62*, 32.

(10) Chan, M.-C.; Okumura, M.; Gabrys, C. M.; Xu, L.-W.; Rehfuss, B. D.; Oka, T. *Physical Review Letters* **1991**, *66*, 2060.

(11) Momose, T. *Journal of Chemical Physics* **1997**, *109*, 15.

(12) Fajardo, M. E.; Tam, S. *Journal of Chemical Physics* **1998**, *108*, 4237.

(13) Oka, T. *Annual Review of Physical Chemistry* **1993**, *44*, 299.

(14) Cox, K.E., Williamson, K.D. *Hydrogen: Its Technology and Implications* **1977,** CRC Press

(15) Souers, P. C. *Hydrogen Properties for Fusion Energy* **1986,** University of California Press.

(16) Welsh, H. L. *M.T.P International Review of Science, Physical chemistry* **1972**, 33.

(17) Nosanow, L. H. *Physical Review* **1966**, *146*, 120.

(18) Brooks, R. L. *Journal of Chemical Physics* **1986**, *85*, 1247.

(19) Tam, S.; Fajardo, M. E. *Journal of Chemical Physics* **1999**, *111*, 4191.

(20) Hoshina, H.; Kato, Y.; Morisawa, Y.; Wakabayashi, T.; Momose, T. *Chemical Physics* **2004**, *300*, 69.

(21) Hoshina, H.; Fushitani, M.; Momose, T.; Shida, T. *Journal of Chemical Physics* **2004**, *120*, 3706.

(22) Pauling, L. *Physical Review* **1930**, *36*, 430.

(23) Momose, T.; Katsuki, H.; Hoshina, H.; Sogoshi, N.; Wakabayashi, T.; Shida, T. *Journal of Chemical Physics* **1997**, *107*, 7717.

(24) Abe, H.; Yamada, K. M. T. *Structural Chemistry* **2003**, *14*, 211.

(25) Brus, L. E.; Bondybey, V. E. *Journal of Chemical Physics* **1976**, *64*, 71.

(26) Chan, M.-C. *Ph. D. dissertation, The University of Chicago* **1991**.

(27) Momose, T.; Miki, M.; Wakabayashi, T.; Shida, T.; Chan, M. C.; Lee, S. S.; Oka, T. *Journal of Chemical Physics* **1997**, *107*, 7707.

(28) Yoshioka, K.; Anderson, D. T. *Journal of Chemical Physics* **2003**, *119*,

4731.

(29) Tam, S.; Fajardo, M. E. *Review of Scientific Instruments* **1999**, *70*, 1926.

(30) A, S. M.; J, H. R. *Physical review letters* **2000**, *85*, 5595.

(31) Andrews, L.; Xuefeng, W. *Review of Scientific Instruments* **2004**, *75*, 3039.

(32) Momose, T.; Fushitani; sect; Mizuho; Hoshina; para; Hiromichi *International Reviews in Physical Chemistry* **2005**, *24*, 533.

(33) Griffiths, P. R.; Haseth, J. A. d. *Fourier Transform Infrared Spectroscopy* **1986**, New York:Wiley-Interscinece

(34) Yu, C.-F.; Whaley, K. B.; Hogg, C. S.; Sibener, S. J. *Journal of Chemical Physics* **1985**, *83*, 4217.

(35) Sears, V. F.; Kranendonk, J. V. *Canadia Journal of Physics* **1964**, *42*, 980.

(36) Gush, H. P.; Hare, W. F. J.; Allin, E. J.; Welsh, H. L. *Canadia Journal of Physics* **1960**, *38*, 176.

(37) Tam, S.; Fajardo, M. E. *Applied Spectroscopy* **2001**, *55*, 1634.